ISSN 0036-0295, Russian Metallurgy (Metally), Vol. 2019, No. 8, pp. 781–786. © Pleiades Publishing, Ltd., 2019.
Russian Text © The Author(s), 2019, published in Rasplavy, 2019, No. 2, pp. 156–166.

Binding Energies in the Molten M–Al–Zr–O–F Systems (M = Li, Na, K)

A. S. Vorob'ev[a], A. V. Suzdal'tsev[a, *], and A. E. Galashev[a]

[a] *Institute of High-Temperature Electrochemistry, Ural Branch, Russian Academy of Sciences, Yekaterinburg, 620990 Russia*
**e-mail: suzdaltsev_av@mail.ru*

Received July 20, 2018; revised July 29, 2018; accepted August 5, 2018

Abstract—The binding energies in complex anions formed from the components Al–F, Zr–F, Al–O–F, and Zr–O–F are calculated by the ab initio Siesta molecular dynamics simulation. The formation of the anions is related to the dissolution of the ZrO_2 and Al_2O_3 oxides in $MF–AlF_3$ (M = Li, Na, K) fluoride melts. The influence of the element compositions of the anions and the cation from the second coordination sphere on the binding energies of the complex anions is determined. Among the oxygen-containing anions, the $Al_2O_2F_6^{2-}$ and $Zr_2O_2F_6^{2-}$ anions are shown to be most stable. Under identical conditions, the anions formed by zirconium are characterized by the lowest energy of the determining bond. The replacement of the cation in the second coordination sphere in the series from K to Li decreases the binding energy in the $M_2Al_2O_2F_6$ and $M_2Zr_2O_2F_6$ anions.

Keywords: oxide–fluoride melt, anions, zirconium, aluminum, molecular dynamic simulation, binding energy, stability

DOI: 10.1134/S0036029519080160

INTRODUCTION

It is desirable that cast aluminum would have a fine-grained structure, because the latter improves the mechanical properties and service characteristics due to the higher homogeneity and decreased porosity. Grain grinding in aluminum and its alloys is usually conducted by the addition of metal-grain grinders. Transition metals, such Ti, Sc, Zr, V, and Cr, are used as grain grinders for aluminum and aluminum alloys [1–3]. In particular, very insignificant additions of zirconium and aluminum (not more than 0.28 wt %) give very fine grains close in sizes. Zirconium can be introduced into molten aluminum before casting by the addition of zirconium salts (K_2ZrF_6, $NaZrF_4$) into a coating salt flux [4, 5]. However, the use of this chemical compound results in unpredictable and detrimental sequences, such as the evolution of gaseous fluoride components (AlF_3, ZrF_4) to atmosphere.

The methods of preparing alloys and Al–Zr master alloys using ZrO_2 oxide seem to be more promising. In particular, there the aluminothermic reduction of ZrO_2 was studied in the following systems: $CaO–CaF_2$ at 1600°C [6, 7], $KClO_3–S$ or $NaNO_3–S$ at 1725°C [8], and $KF–AlF_3$ at 750–800°C [9, 10]. Owing to the high yield of zirconium (up to 99.5%), low temperature, and possibility to organize the permanent production of alloys and Al–Zr master alloys with the zirconium content up to 15 wt %, it seems most energetically efficient to reduce ZrO_2 oxide by aluminum under electrolysis conditions in oxide–fluoride melts based on the $KF–AlF_3$ and $NaF–AlF_3$ systems with additions of Al_2O_3 and ZrO_2 oxides [11–14]. However, the reduction kinetics and the synthesis parameters depend, to a great extent, on the composition of zirconium complexes that form upon the dissolution of ZrO_2 in an oxide–fluoride melt.

The search for alternative methods for the electrolytic preparation of aluminum resulted in the necessity to study the stability of aluminum oxychloride and aluminum oxide [15] and to analyze the role of the fluorine anion in the conventional solubility of alumina in chloride melts [16]. An idea of the possible electrical isolation of aluminum from the chloride–fluoride–oxide melts was also advanced [17]. All the studies suffer from a lack of information on the structures of the formed ionic complexes.

Modeling methods look like very promising tools for obtaining data on the structural and energetic properties and an information about vibrations in complex anions. The use of software for computations in the framework of the density functional theory (DFT) makes it possible to take into account exchange and correlation effects, and the volume of calculations decreases by two orders of magnitude compared to the Hartree–Fock method. All geometry optimizations can be performed without any fixed symmetry using

the DFT method. The geometry optimization of the anions shows that an aluminum atom is always pentacoordinated; i.e., it exists in the environment of four fluorine atoms and one oxygen atom [17].

To compare the energies of all complexes, it is preferable to calculate their binding energies. Based on these calculations, one can directly compare the relative stabilities of the complexes. The aluminum complexes were comprehensively examined [17, 18] due to which the data obtained in the present work can be verified.

The purpose of this work is to reveal the most stable complex compounds in the molten M–Al–Zr–O–F systems (M = Li, Na, and K) by the calculation of the binding energy and to compare the data obtained with the binding energies of the aluminum complexes.

A significant number of scientific technical problems about the influence of this or another factor on the processes of electrolytic aluminum production has recently been solved using model calculations [19–21]. Therefore, along with the extension of concepts on complex formation in the KF–Al_3, NaF–Al_3, and LiF–Al_3 melts with additions of Al_2O_3 and ZrO_2, the data obtained in this work can be used for modeling the processes that occur in a melt and at the electrodes in the traditional cryolite–alumina melt with additions (impurities) of LiF, KF, and ZrO_2.

CALCULATION PROCEDURE

The DFT method [22, 23] is the most efficient approach to the calculation of binding energies and crystal lattice dynamics. The essence of the method is described by the following theorem: the energy of the ground state of the system of interacting electrons in the atomic nuclei field is single-valued electron density functional $\rho(r)$ (Kohn–Sham functional). When $\rho(r)$ is varied, the functional reaches its extreme (minimum) equal to the energy of the ground state of the system on the valid electron density distribution. This statement can be written as the following condition:

$$\frac{\delta E[\rho]}{\delta \rho} = 0. \quad (1)$$

To calculate the total energy of the system, it is necessary to determine a set of wave functions $\Psi_i(\mathbf{r})$ that minimize the Kohn–Sham functional. They are determined from Eq. (1). Exchange correlation potential $V_{XC}(\mathbf{r})$ can be determined hrough the functional derivative

$$V_{XC}(\mathbf{r}) = \frac{\delta E_{XC}[\rho]}{\delta \rho(\mathbf{r})} = \frac{\partial[\rho(\mathbf{r})\varepsilon_{XC}(\mathbf{r})]}{\partial \rho(\mathbf{r})}, \quad (2)$$

where $\varepsilon_{XC}(\mathbf{r}) = \varepsilon_{XC}^{\text{hom}}[\rho(\mathbf{r})]$; and $\varepsilon_{XC}^{\text{hom}}$ is the exchange correlation energy of the homogeneous electron gas with density ρ per electron.

As a result, we have the local density approximation in which the density of the exchange correlation energy at the point $\mathbf{r}$ is equal to the exchange correlation energy density in the homogeneous electron gas with the same density $\rho(\mathbf{r})$.

The generalized gradient approximation (GGA) is an exact approximation for the exchange correlation energy. In this case, the exchange correlation functional depends not on the density only but also on its first spatial derivative as follows:

$$E_{XC}[\rho] = \int \rho(\mathbf{r})\varepsilon_{XC}[\rho(\mathbf{r})\nabla\rho(\mathbf{r})]d^3\mathbf{r}. \quad (3)$$

The specific form of the GGA approximation proposed by Perdew et al. [24] is often used for the calculation of the electronic properties of solids. We used the standard procedure of orbital expansion over a basis set, and planar waves were chosen as the basis set. In this case, the wave functions can be written as the expansion

$$\Psi_i(\mathbf{r}) = \sum_G C_{i,k+G} \exp[i(\mathbf{k} + \mathbf{G}) \cdot \mathbf{r}]. \quad (4)$$

As a result, the Kohn–Sham equations take the form of the following system of linear algebraic equations determining the $C_{i,k+G}$ coefficients:

$$\sum_G \left[\frac{\hbar^2}{2m}|\mathbf{k} + \mathbf{G}|^2 \delta_{GG'} + V_{\text{ion}}(\mathbf{G} - \mathbf{G}') + V_{\text{H}}(\mathbf{G} - \mathbf{G}') + V_{XC}(\mathbf{G} - \mathbf{G}')\right] C_{i,k+G'} = \varepsilon_i C_{i,k+G}, \quad (5)$$

where V_{ion} is the static electronic–ionic potential, V_{H} is the Hartree potential for electrons, and ε_i is the eigenvalue of the Kohn–Sham equation [23]. This system of equations is a standard problem of linear algebra for finding eigenvalues.

The calculations were performed using the Siesta software package. Geometric optimization was performed using GGA in the Perdew–Burke–Ernzerhof form by the diagonalization method without fixing coordinates. Three-exponential basis set and polarization functions were used in all calculations. Network cutting equal to 300 Ry was applied in the inverse spatial expansion of the charge density. The convergence criterion for the energy of the self-consistent field (SCF) cycle was chosen to be 10^{-3} eV. The binding energies were calculated using the equation

$$E_{\text{bind}} = E_{\text{OMF}} - N_{\text{M}}E_{\text{M}} - N_{\text{F}}E_{\text{F}} - N_{\text{O}}E_{\text{O}}, \quad (6)$$

where E_{OMF}, E_{M}, E_{F}, and E_{O} are the total energies of the complex, single metal atom (Al^{3+}, Zr^{4+}), fluorine (F^-) ion, and oxygen (O^{2-}) anion, respectively, and N_{M}, N_{F}, and N_{O} are the numbers of metal, fluorine, and oxygen atoms, respectively, in the system.

All obtained binding energies for the complexes formed by Al and Zr cations are presented in Table 1

Table 1. Binding energies (eV) for various Al- and Zr-containing complexes (x is the number of fluorine atoms in a complex)

Complex	x								
	1	2	3	4	5	6	7	8	9
AlF_x^{z-}	–	–	–65.0	–69.5	–69.6	–63.0	–	–	–
ZrF_x^{z-}	–	–	–	–92.0	–98.6	–97.5	–	–	–
$AlOF_x^{z-}$	–73.9	–80.0	–79.7	–72.4	–	–	–	–	–
$ZrOF_x^{z-}$	–89.8	–103.1	–109.1	–107.7	–	–	–	–	–
$Al_2OF_x^{z-}$	–	–	–	–142.7	–149.1	–151.0	–146.7	–138.4	
$Zr_2OF_x^{z-}$	–	–	–	–173.3	–189.9	–202.2	–207.6	–209.3	–206.3
$Al_2O_2F_x^{z-}$	–	–153.4	–158.4	–158.6	–156.2	–150.8	–	–	–
$Zr_2O_2F_x^{z-}$	–	–183.8	–199.5	–209.5	–219.2	–220.1	–216.5	–	–
$AlZrOF_x^{z-}$	–	–	–	–160.1	–172.5	–179.1	–180.4	–176.3	–171.1
$AlZrO_2F_x^{z-}$	–	–170.9	–181.5	–186.4	–190.7	–186.2	–177.3	–	–

together with the binding energies of the hypothetical complexes formed simultaneously by Zr and Al.

RESULTS AND DISCUSSION

Binding energies in the AlF_x^{z-} *and* ZrF_y^{z-} *Complexes*

The binding energy is equivalent to the energy necessary for disintegrating the whole system into components. The system bound in the complex usually has a lower potential energy than the sum of its components. In other words, the parts of the system are retained together due to this energy. It often means that the energy is evolved when the bound state is formed. The compound is stable if the overall potential energy of its components is negative. In this work, we will follow this definition of the binding energy (see Eq. (6)).

The dependences of the binding energies obtained for the AlF_x^{z-} and ZrF_x^{z-} complexes are shown in Fig. 1. The binding energy of the AlF_4^- complex obtained earlier [17] is also presented. An insignificant deviation of the values of E_{bind} is caused by the use of the program package and the exchange correlation potential differed from those applied earlier [17].

The following conclusions can be drawn on the basis of the dependences shown in Fig. 1. First, AlF_4^- (–69.51 eV) and AlF_5^{2-} (–69.56 eV) are the most stable among all aluminum complexes presented, which is consistent with the published data [18]. The result obtained earlier [18] indicates that the molten $MF–AlF_3$ (M = Li, Na, K) systems mainly consist of complexes AlF_4^- and AlF_5^{2-}. Second, the zirconium complexes are characterized by a stronger bond (more negative binding energy) than similar aluminum complexes. Third, the ZrF_5^- complex is characterized by the strongest bond and, correspondingly, the lowest energy characterizing the bond (–98.57 eV).

Binding Energies of the $X_2O_2F_y^{z-}$ *Complexes*

The binding energies of the $X_2O_2F_y^{z-}$ complexes (where X_2 is the complexing agent (Zr_2, Al_2, and ZrAl), and y is the number of fluorine atoms) are

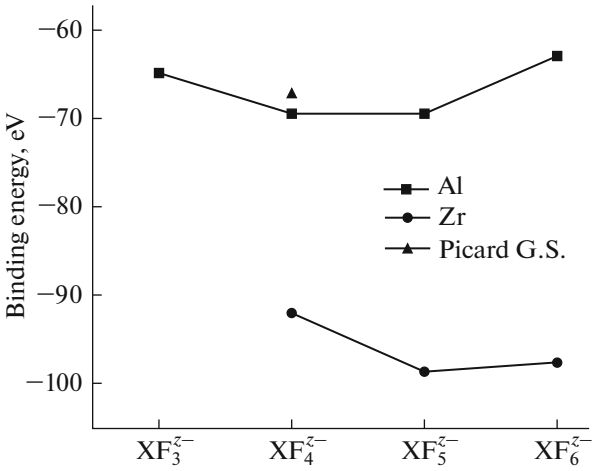

Fig. 1. Calculated binding energies for (■) AlF_x and (●) ZrF_x complex anions. The data for AlF_x are compared with (▲) data in [17].

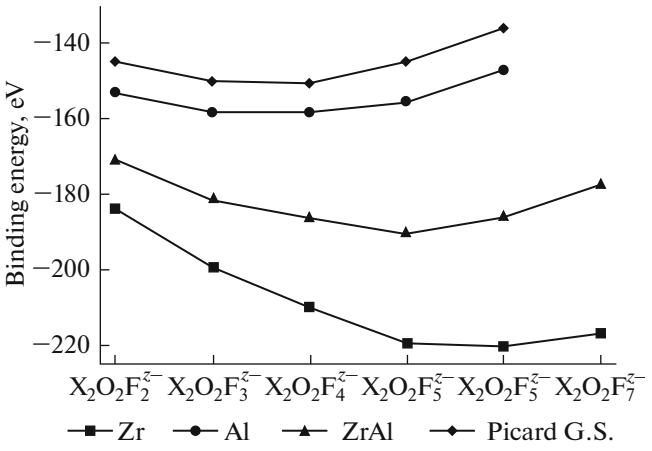

Fig. 2. Binding energies for the $X_2O_2F_y^{2-}$, complexes, where X_2 is (●) Zr_2, (■) Al_2, or (▲) ZrAl.

shown in Fig. 2. The binding energies obtained for the $Al_2O_2F_y^{z-}$ aluminum complexes are lower (by 5–7%) than the previously determined binding energies of the corresponding complexes [17]. However, the position of the binding energy minimum and the dependence for this complex coincide with similar characteristics obtained earlier [17].

The following conclusions can be made on the basis of the dependences shown in Fig. 2. First, the $Zr_2O_2F_6^{2-}$ complex anion is characterized by the strongest bond (−220.14 eV). Second, a comparison of the binding energies for the $X_2O_2F_y^{z-}$ complexes (where $X_2 = Al_2$, Zr_2, and ZrAl) at equal y shows that the bonds become weaker (the absolute value of binding energy increases) on going from the zirconium complexes to the mixed aluminum–zirconium compounds and further to the aluminum complexes. As can be seen from Table 1, this correlation is valid for all cases under study. Third, the binding energy minima were observed in the y range from 4 to 6 for all considered groups of the complexes.

Structures of the Most Stable Complexes

The 3D structures of four zirconium compounds, $ZrOF_3^-$, $Zr_2OF_8^{2-}$, $Zr_2O_2F_6^{2-}$, and $Li_2Zr_2O_2F_6$, are displayed in Fig. 3. These compounds are most stable in their group and have the lowest binding energies, which is seen from the data in Table 1. The bond lengths calculated for these compounds are given in Table 2. The following conclusions can be made from these data: (1) each of the considered compounds has pronounced symmetry, (2) the Zr^{4+} ion is the center in all compounds, and (3) the Zr–F and Zr–O bond lengths in all compounds considered are fairly close.

Influence of the Second Coordination Sphere

Figure 4 shows the influence of the second coordination sphere (chemical potential of the cation in the system) on the binding energy in the $M_2Al_2O_2F_6$ and $M_2Zr_2O_2F_6$ (M = K, Na, Li) systems. As can be seen from Fig. 4, the insertion of M atoms decreases the binding energy. This fact is explained by a change in the geometric structures of these complexes (see Fig. 2), which can be seen for compound $Li_2Zr_2O_2F_6$ as an example. The hypothetical joining of the alkaline metal and compound $Zr_2O_2F_6^{2-}$ appreciably decreases the binding energy of the complex. The strongest decrease in the binding energy is observed for the insertion of Li atoms into the complex.

Based on the data in Fig. 4, the following conclusions can be drawn. First, the correlation between the binding energies for the zirconium and aluminum compounds is retained: the zirconium complexes also have a lower binding energy than similar aluminum compounds. Second, each additional cation introduces its change to the binding energy: the addition of Li is accompanied by the lowest binding energy, and K is characterized by the highest binding energy. Third,

Table 2. Bond lengths (A) for the $ZrOF_3^-$, $Zr_2OF_8^{2-}$, $Zr_2O_2F_6^{2-}$, and $Zr_2Li_2O_2F_6$ complexes

	Zr–Zr	Zr–F	Zr–O	F–F	F–O	O–O	F–Li
$ZrOF_3^-$	–	2.07	1.88	2.88	3.09	–	–
$Zr_2OF_8^{2-}$	–	2.02	1.99	2.73	3.13	–	–
$Zr_2O_2F_6^{2-}$	3.10	2.03	1.97	2.87	2.94	2.65	–
$Li_2Zr_2O_2F_6$	3.07	1.98	1.92	2.93	2.84	2.676	1.80

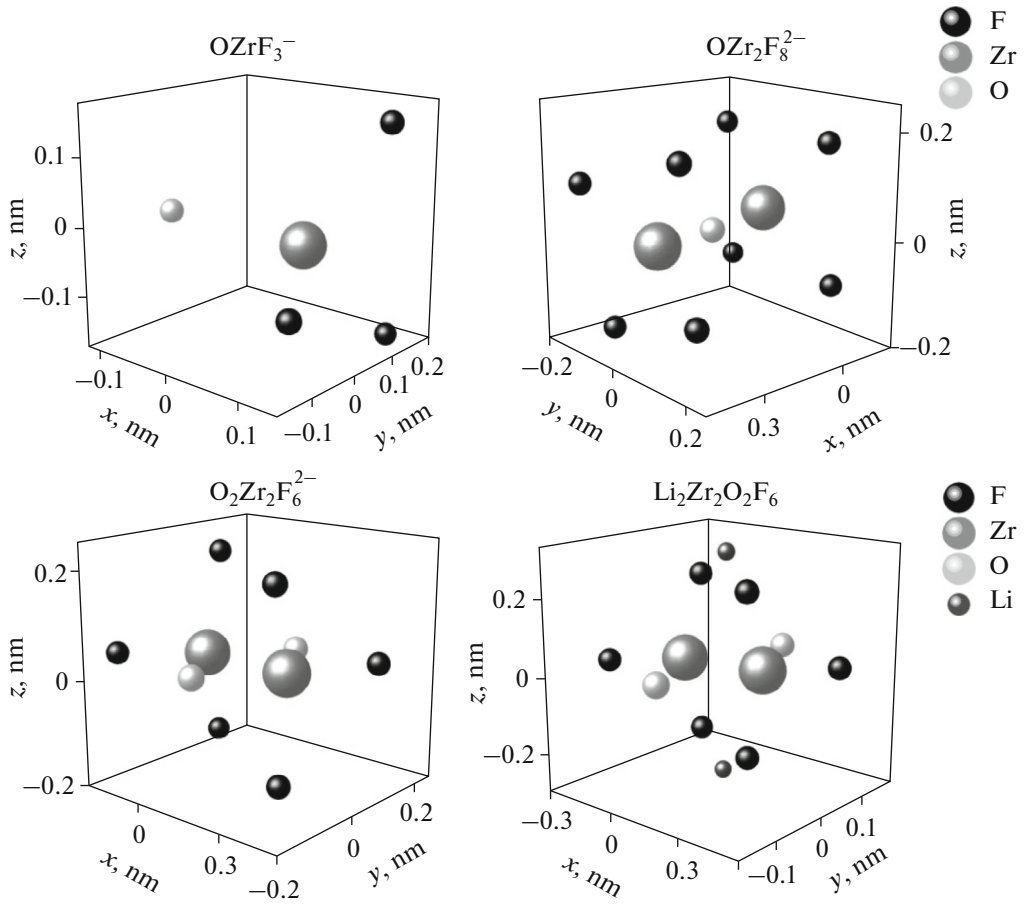

Fig. 3. 3D structures of some complex anions.

the lithium-containing complexes are most stable: the binding energy of the aluminum compound ($Li_2Al_2O_2F_6$) is –182.153 eV and that of the zirconium compound ($Li_2Zr_2O_2F_6$) is –235.705 eV.

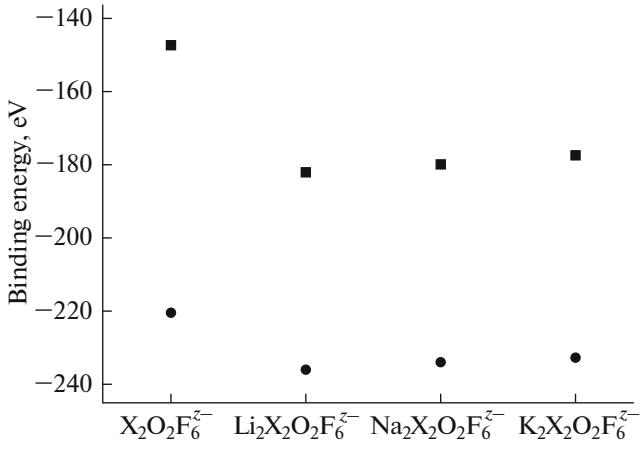

Fig. 4. Binding energies for the $M_2Al_2O_2F_6$ and $M_2Zr_2O_2F_6$ (M = K, Na, Li; X = (●) Zr or (■) Al) complexes calculated taking into account the geometric neighbors from the second coordination sphere.

CONCLUSIONS

This study extends the concepts on the complex formation processes in the melts based on the KF–NaF–AlF_3–ZrO_2 systems used for the production of alloys and Al–Zr master alloys. The obtained results can briefly be generalized as follows.

(1) Compound $Zr_2O_2F_6^{2-}$ has the lowest binding energy of all zirconium complexes under study if the influence of the second coordination sphere is neglected.

(2) The zirconium complexes are the most stable compared to similar aluminum–zirconium and aluminum complexes.

(3) The binding energy in the compound with two complexing agents Al and Zr is lower than that in similar aluminum complexes.

(4) The addition of Li^+, Na^+, or K^+ cations to compound $X_2O_2F_6^{z-}$, where $X_2 = Al_2$ or Zr_2, increases the stability of the system for both the zirconium and aluminum complexes. The Li-containing complexes are characterized by the lowest binding energy, and the complexes containing K have the highest binding energy.

(5) In all groups of the systems, there are complexes with the lowest binding energy indicated by a minimum in the corresponding energy dependence.

(6) Compound $Li_2Zr_2O_2F_6$ shows the strongest bond (–235.705 eV) among the complexes presented in this work.

REFERENCES

1. D. V. Ogorodov, D. A. Popov, and A. V. Trapeznikov, "Methods of preparing an Al–Zr master alloy (review)," Trudy VIAM, No. 11, 2–11 (2015).
2. K. E. Knipling, D. N. Seidman, and D. C. Dunand, "Ambient- and high-temperature mechanical properties of isochronally aged Al–0.06Sc, Al–0.06Zr, and Al–0.06Sc–0.06Zr (at %) alloys," Acta Mater. **59**, 943–954 (2011).
3. M. I. Gasik, N. P. Lyakishev, and B. I. Emlin, *Theory and Practice of Manufacturing Ferroalloys* (Metallurgiya, Moscow, 1988).
4. S. P. Yatsenko, B. V. Ovsyannikov, M. A. Ardashev, and A. N. Sabirzyanov, "Carbonization preparation of "master alloy" from fluoride–chloride melts," Rasplavy, No. 5, 29–36 (2006).
5. V. I. Napalkov and S. V. Makhov, *Alloying and Modification of Aluminum and Magnesium* (MISIS, Moscow, 2002).
6. S. A. Krasikov, S. N. Agafonov, V. P. Chentsov, and E. M. Zhilina, "The effect of phase formation on the character of interphase interactions during aluminothermic reduction of zirconium from its dioxide," Rasplavy, No. 2, 60–64 (2015).
7. S. N. Agafonov, S. A. Krasikov, A. A. Ponomarenko, and L. A. Ovchinnikova, "Phase formation in the aluminothermic reduction of ZrO_2," Neorg. Mater., **48**, 927–934 (2012).
8. J. M. Juneja, "Preparation of aluminium–zirconium master alloys," Ind. J. Eng. Mater. Sci. **9**, 187–190 (2002).
9. P. S. Pershin, A. A. Filatov, A. V. Suzdal'tsev, Yu. P. Zaikov, "Aluminothermic preparation of Al–Zr alloys in the $KF–AlF_3$ melt," Rasplavy, No. 5, 413–421 (2016).
10. P. S. Pershin, A. A. Kataev, A. A. Filatov, A. V. Suzdal'tsev, and Yu. P. Zaikov, "Synthesis of Al–Zr alloys via ZrO_2 aluminium-thermal reduction in $KF–AlF_3$-based melts," Met. Mater. Trans. B **48**, 1962–1969 (2017).
11. A. A. Filatov, P. S. Pershin, A. Yu. Nikolaev, and A. V. Suzdal'tsev, "Synthesis of Al–Zr alloys and master alloys during the electrolysis of $KF–NaF–AlF_3–ZrO_2$ melts," Tsvetn. Met., No. 11, 27–31 (2017).
12. E. Kubinakova, V. Danielik, and J. Hives, "Advanced technology for Al–Zr alloy synthesis: Electrochemical investigation of suitable low-melting electrolytes," J. Alloys Compd. **738**, 151–157 (2018).
13. A. A. Suzdal'tsev, A. A. Filatov, A. Yu. Nikolaev, A. A. Pankratov, N. G. Molchanova, and Yu. P. Zaikov, "Extraction of scandium and zirconium from their oxides during the electrolysis of oxide–fluoride melts," Russ. Metall. (Metally), No. 1, 5–13 (2018).
14. A. A. Filatov, P. S. Pershin, A. V. Suzdaltsev, A. Yu. Nikolaev, and Yu. P. Zaikov, "Synthesis of Al–Zr master alloys via the electrolysis of $KF–NaF–AlF_3–ZrO_2$ melts," J. Electrochem. Soc. **165** (2), E28–E34 (2018).
15. G. S. Picard, F. Seon, and B. Tremillon, "Oxoacidity reactions in molten lithium chloride + potassium chloride eutectic (at 470°C): potentiometric study of the equilibria of exchange of oxide ion between aluminum(III) systems and carbonate and water systems," J. Electroanal. Chem. Interfac. Electrochem. **102** (1), 65–75 (1979).
16. G. S. Picard, F. Seon, B. Tremillon, and Y. Bertaud, "Effect of the addition of fluoride on the conditional solubility of alumina in lithium chloride–potassium chloride eutectic melt," Electrochim. Acta, **25** 1453–1462 (1980).
17. G. S. Picard, F. C. Bouyer, M. Leroy, Y. Bertaud, and S. Bouvet, "Structures of oxyfluoroaluminates in molten cryolite–alumina mixtures investigated by DFT-based calculations," J. Mol. Struct. (Theochem) **368**, 67–80 (1996).
18. E. Robert, J. E. Olsen, V. Danek, E. Tixhon, T. Ostvold, and B. Gilbert, "Structure and thermodynamics of alkali fluoride–aluminum fluoride–alumina melts. Vapor pressure, solubility, and Raman spectroscopic studies," J. Phys. Chem. B **101**, 9447–9456 (1997).
19. R. J. Thorne, C. Sommerseth, A. P. Ratvik, S. Rorvik, E. Sandnes, L. P. Lossius., H. Ling, and A. M. Svensson, "Correlation between coke type, microstructure, and anodic reaction overpotential in aluminium electrolysis," J. Electrochem. Soc. **162** (12), E296–E306 (2015).
20. A. Y. Galashev and O. R. Rakhmanova, "Computer modeling of oxygen migration accompanying aluminum production," Lett. Mater. **7** (4), 373–379 (2017).
21. A. Y. Galashev and O. R. Rakhmanova, "Computer study of oxygen release from Al melts," Model. Simul. Mater. Sci. Eng. **26**, 025003 (2017).
22. P. Hohenberg and W. Kohn, "Inhomogeneous electron gas," Phys. Rev. B **136**, 864–871 (1964).
23. W. Kohn and L. J. Sham, "Self-consistent equations including exchange and correlation effects," Phys. Rev. A **140**, 1133–1138 (1965).
24. J. P. Perdew, K. Burke, and M. Ernzerhof, "Generalized gradient approximation made simple," Phys. Rev. Lett. **77**, 3865–3868 (1996).

Translated by E. Yablonskaya